PERGAMON

Solid State Communications 118 (2001) 351–354

solid state communications

www.elsevier.com/locate/ssc

Ultra-long single crystalline nanoribbons of tin oxide

Z.R. Dai, Z.W. Pan, Z.L. Wang*

School of Materials Science and Engineering, Georgia Institute of Technology, Atlanta, GA 30332-0245, USA

Received 12 February 2001; received in revised form 28 February 2001; accepted 7 March 2001 by D.E. Van Dyck

Abstract

Novel nanoribbons of single crystalline SnO_2 have been successfully synthesized by simple thermal evaporation of SnO or SnO_2 powders at high temperatures. Field emission scanning electron microscopy (FE-SEM) and transmission electron microscopy (TEM) show that the nanoribbons are structurally perfect and uniform, with widths of 30–200 nm, width-to-thickness ratio of ~5–10, and lengths of several hundred micrometers to a few millimeters. X-ray diffraction (XRD) and energy dispersive X-ray spectroscopy (EDS) analysis indicate that the nanoribbons have the same crystal structure and chemical composition found in the rutile form of SnO_2. Electron diffraction (ED) and high resolution transmission electron microscopy (HRTEM) reveal that the nanoribbons grow along the [101] crystal direction and they are bounded by (010)/(0$\bar{1}$0) and (10$\bar{1}$)/($\bar{1}$01) crystal facets.

PACS: 68.70.+w; 68.75.+w; 81.10.Bk

Keywords: A. Nanostructures; A. Semiconductors; B. Nanofabrications; B. Crystal growth; C. Scanning and transmission electron microscopy

1. Introduction

One-dimensional (1D) nanostructures, such as nanotubes and nanowires, have attracted extraordinary attention for their potential applications in device and interconnect integration in nanoelectronics and molecular electronics [1–5]. Synthesis of 1D nanostructures has been demonstrated for cylindrical carbon nanotubes [6,7] and in semiconducting nanowires such as Si[8–11], Ge[12], GaAs[13], GaN[14], etc. The semiconducting metal oxide SnO_2 is a key functional material that has been extensively used for gas sensors [15,16] and optoelectronic devices [17,18], usually in a form of dispersed particles or condensed thin films. Synthesis of wire-like nanostructures of SnO_2 has not been reported before the present study.

2. Experiment

The experimental apparatus used for the synthesis consists of a horizontal tube furnace, an alumina tube, a rotary pump system and a gas supply and control system. Commercial (Alfa Aesor) SnO or SnO_2 powders with a purity of 99.9% (metal basis) was used as the source material that was placed in an alumina crucible, the crucible being located at the center of the alumina tube. Several alumina strip plates (60 × 10 mm) were placed downstream one by one inside the alumina tube, which acted as substrates for collecting the growth products. After evacuating the alumina tube to $\sim 2 \times 10^{-3}$ Torr, thermal evaporation was conducted at 1000°C for SnO powders or 1350°C for SnO_2 powders for 2 h under a pressure of 300 Torr and Ar gas flow of rate 50 sccm (standard cubic centimeters per minute). A white-color fuzzy looking product was collected in a narrow region downstream, where the temperature was in the range of 900–950°C. A similar product was obtained in the same temperature zone regardless of whether the source material was SnO or SnO_2. The as-synthesized product was characterized by XRD, FE-SEM, TEM, HRTEM and EDS.

3. Results and discussion

The as-synthesized product consists of a large quantity of ultra-long wire-like nanostructures (Fig. 1) and a few Sn particles as identified by EDS. Typically, the wire-like nanostructures are several hundred micrometers in length. Some of them even have lengths on the order of millimeters.

* Corresponding author.
E-mail address: zhong.wang@mse.gatech.edu (Z.L. Wang).

0038-1098/01/$ - see front matter
PII: S0038-1098(01)00122-3

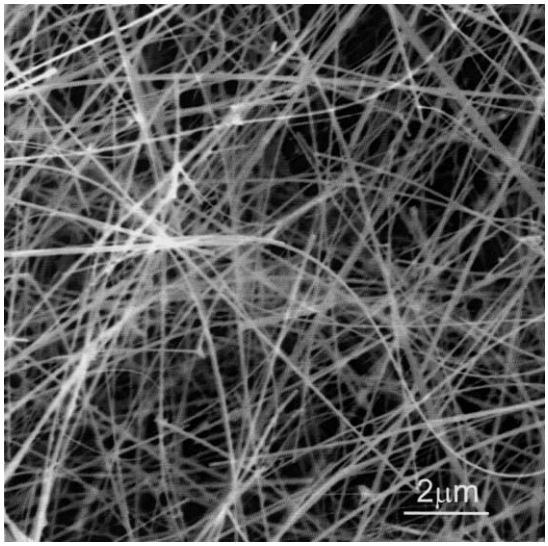

Fig. 1. FE-SEM image of as-synthesized SnO_2 nanoribbons showing high purity, high yield, and ultra-long and uniform morphology.

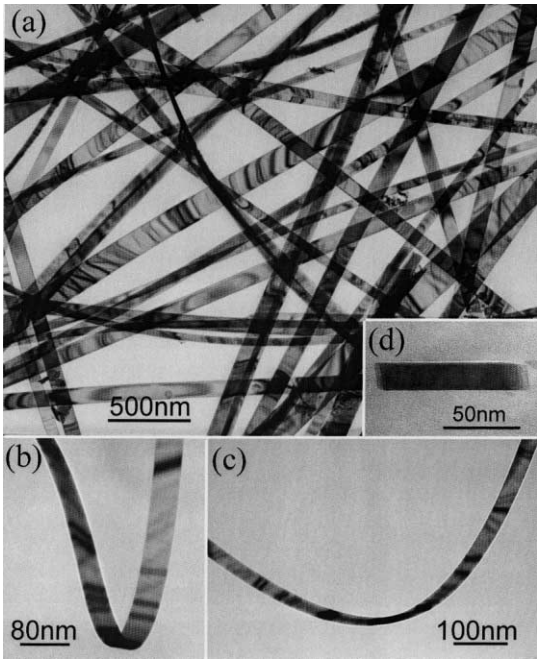

Fig. 2. (a) TEM bright-field image of SnO_2 nanoribbons, showing strain contrast introduced by the bending of the nanoribbons. Each nanoribbon is singly crystalline without dislocation; (b) and (c) display the characteristic features of SnO_2 nanoribbons. (d) Cross-sectional TEM image of a nanoribbon. The specimen was prepared by slicing nanoribbons embedded in epoxy with an ultramicrotome.

The chemical composition of the nanostructures is determined to be SnO_2. XRD analysis indicates that the as-synthesized SnO_2 nanostructures have the rutile structure, with lattice constants $a = 4.732$ Å and $c = 3.184$ Å, which are consistent with those of bulk SnO_2 [19].

The geometrical shape of the SnO_2 wire-like nanostructures has been determined by TEM imaging. Shown in Fig. 2(a) is a bright-field TEM image, which displays a ripple-type contrast for most of the nanostructures, indicating the presence of strain. The profile of the fringes implies that the geometrical shape of the wire-like nanostructures is likely to be a ribbon. The ribbon shape is further confirmed by the images given in Fig. 2(b) and (c), where the twist of ribbons is evident. Therefore, the as-synthesized wire-like nanostructures are nanoribbons of SnO_2, with a geometrical configuration different from the cylindrical 1D nanostructures reported earlier.

The width and thickness of each SnO_2 nanoribbon are rather uniform, and the variation of the width among different nanoribbons is 30–200 nm. The thickness of the SnO_2 nanoribbons varies with their widths. The width-to-thickness ratio of the nanoribbons has been determined by cross-sectional TEM imaging to be 5–10 (Fig. 2(d)). Electron diffraction and imaging indicate that each SnO_2 nanoribbon is single crystalline, structurally uniform and dislocation-free, but do not exclude point defects.

An HRTEM image recorded near the edge of a SnO_2 nanoribbon along the direction perpendicular to the wide surface of the nanoribbon is given in Fig. 3, where the inset is the corresponding electron diffraction pattern. The surface of the nanoribbon is clean and abrupt on an atomic scale with some atom-high steps and point defects, as shown

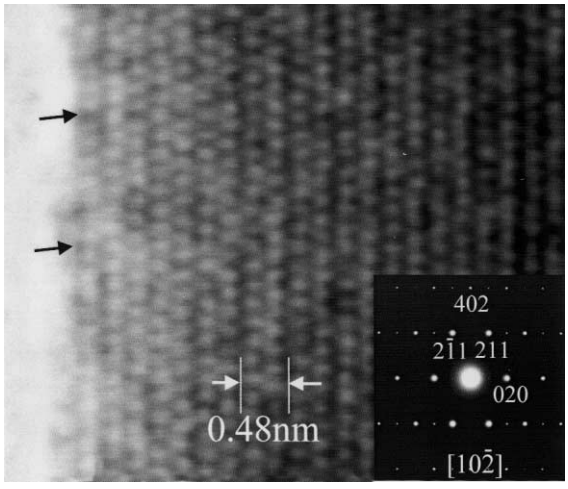

Fig. 3. HRTEM image recorded near the edge of a SnO_2 nanoribbon along the direction perpendicular to the wide surface of the nanoribbon, where columns of Sn cations are clearly resolved. The inset shows the corresponding electron diffraction pattern clearly indicating the crystallographic planes enclosing the nanoribbon as well as the growth plane and direction.

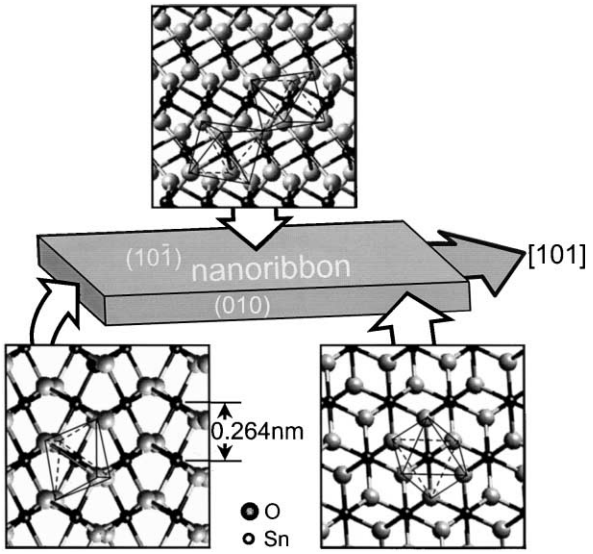

Fig. 4. Structural model of the SnO_2 nanoribbon, where the atomic arrangements at the top, side and growth surface are illustrated. The coordination octahedra of the Sn cations are marked.

by the black arrowheads, and there is no amorphous layer covering on the surface. The SnO_2 nanoribbons, however, are sensitive to electron beam irradiation at 400 kV, resulting in the formation of some point defects. The electron diffraction pattern is indexed to be [10$\bar{2}$] zone axis of the rutile structured SnO_2 crystal. That means that the normal direction of the wide surface of the ribbon corresponds to a [10$\bar{2}$] and the surface plane is close to a (10$\bar{1}$) crystallographic plane. The narrow side surface of the nanoribbon is the (010) crystallographic plane. The axial growth plane is (201) and the growth direction is close to [101].

A schematic structural model of the nanoribbon is shown in Fig. 4. The (10$\bar{1}$) wide surface of the nanoribbon corresponds to the closest packing plane for the Sn cations in the rutile structure, while the (010) narrow surface is parallel to the closest packed plane for the O anions. It is known that the close-packed ionic planes have relatively lower surface energies, resulting in their preference to be the side surfaces of the as-growing nanoribbons. On the other hand, the growth plane (201) of the nanoribbon may have a relatively higher surface energy, which may lead to a faster growth along the [101] direction, forming a ribbon structure.

The semiconducting oxide (SnO_2) nanoribbons reported here are single crystalline, dislocation free and structurally uniform. They are likely to be an ideal model for the systematic understanding of electrical, thermal, and optical transport processes in one-dimensional semiconducting nanostructures, as well as their response to changes in temperature and partial gas pressure. The semiconducting oxide nanoribbons could be doped with different elements and thus become suitable for the fabrication of nano-size sensors based on the response of single nanoribbons. If successful, this approach may lead to major technological breakthroughs in the field of nano-size sensors and functional devices for low-power consumption and high sensitivity.

Acknowledgements

We thankfully acknowledge the US NSF for its financial support from grants DMR-9733160, the Georgia Tech Electron Microscopy Center for providing the research facilities, and Dr J. Bradley for kindly helping in the preparation of cross-sectional TEM specimens.

References

[1] A.P. Alivisatos, Science 271 (1996) 993.
[2] B.I. Yakobson, R.E. Smalley, Am. Sci. 85 (1997) 324.
[3] C. Dekker, Phys. Today 52 (1999) 22.
[4] J. Hu, T.W. Odom, C.M. Lieber, Acc. Chem. Res. 32 (1999) 435.
[5] C.P. Collier, E.W. Wong, M. Belohradsk, F.M. Raymo, J.F. Stoddart, P.J. Kuekes, R.S. Williams, J.R. Heath, Science 285 (1999) 391.
[6] S. Iijima, Nature 354 (1991) 56.
[7] S. Iijima, T. Ichihashi, Nature 363 (1993) 603.
[8] A.M. Morales, C.M. Lieber, Science 279 (1998) 208.
[9] S.T. Lee, N. Wang, Y.F. Zhang, Y.H. Tang, MRS Bull. 24 (1999) 36.
[10] D.P. Yu, Z.G. Bai, Y. Ding, Q.L. Hang, H.Z. Zhang, J.J. Wang, Y.H. Zou, W. Qian, G.C. Xiong, H.T. Zhou, S.Q. Feng, Appl. Phys. Lett. 72 (1998) 3458.
[11] J.L. Gole, J.D. Scout, W.L. Rauch, Z.L. Wang, Appl. Phys. Lett. 76 (2000) 2346.

[12] Y. Wu, P. Yang, Chem. Mater. 12 (2000) 605.
[13] X. Duan, J. Wang, C.M. Lieber, Appl. Phys. Lett. 76 (2000) 1116.
[14] X. Duan, C.M. Lieber, J. Am. Chem. Soc. 122 (2000) 188.
[15] J. Watson, Sensors and Actuators 5 (1984) 29.
[16] N. Taguchi, US Patent 3 695 848, 1972.
[17] C. Tatsuyama, S. Ichimura, Jpn. J. Appl. Phys. 15 (1976) 843.
[18] A. Aoki, H. Sasakura, Jpn. J. Appl. Phys. 9 (1970) 582.
[19] W.H. Baou, Acta Cryst. 9 (1956) 515.